Multiparametric actuation of bistable plates

Stefano Vidoli[1], Corrado Maurini[2], Amancio Fernandes[2]
[1] *Dipartimento di Ingegneria Strutturale e Geotecnica, La Sapienza Università di Roma, Italy*
E-mail: stefano.vidoli@uniroma1.it

[2]*UPMC Univ Paris 06, UMR 7190, Institut Jean Le Rond d'Alembert, F-75005 Paris, France*
E-mail: maurini@lmm.jussieu.fr, amancio.fernandes@upmc.fr

SUMMARY. Large changes in the shape of a given structural member can be obtained by exploiting geometric nonlinearities or instability phenomena; multistable structures, *i.e.* structures characterized by two or more stable configurations, can undergo large displacements under moderate actuation forces. This feature turns out to be a major advantage for some actuation problems. The study of multistability and of geometrical nonlinear effects in composite plates and shells has recently gained a relevant interest: it is expected that the industrial applications of multistable structures will encompass a large variety of engineering products from micro-electronics systems to human-scale systems. Previous numerical and experimental [5, 8, 11] studies have analyzed the possibility of using a piezoelectric actuation to drive a bistable composite plate from one stable configuration to the other; other recent contributions [10, 13] have investigated the influence of geometry and material properties on the stability properties of shallow shells. We propose new insights regarding both these aspects.

1 INTRODUCTION

In slender structures geometrical effects may induce complex non-linear phenomena. Beams, arches, plates, and shells may exhibit several stable equilibrium configurations very different in shape. The passage from one configuration to another may take place with small deformations and with an approximately linear elastic material behavior. These properties attract the interests of the engineering community to conceive multistable structures able to keep without an external actuation several equilibrium shapes, each one associated to a specific functional regime. Moreover, in multistable structures, small actuation forces may induce great changes in shape by triggering instability phenomena. This allows an efficiently employment of active materials with limited actuation power, such a piezoelectric composites.

The design of morphing multistable structures with embedded actuation is a challenging problem from the theoretical and technologic point of view, demanding to face two main difficulties: 1) taking into account non-linear effects in the design process to obtain a structure with a set of assigned stable equilibrium configurations; 2) conceiving efficient actuation techniques for let the structure pass from one equilibrium configuration to another. The starting point to tackle these issues is a careful study and a syntetic global representation of the non-linear static behavior of the considered class of structures. This may be obtained only on the basis of simplifed low-dimensional model, resuming the foremost qualitative properties of the system.

Thin structures as plates and shells appears as good candidates for shape-changing applications. Multistability is a consequence of the coupling between bending and in-plane extension due to geometrical non-linear effects. The paper is organized in three main parts. In the first part, we derive a simple analytical model for a free orthotropic Föpple-Von Karman plate with inelastic deformations and we present a global synthetic analysis on the dependence of the number and shape of stable

equilibria on the applied inelastic deformations. In the second part, at the light of the global phase portrait as a function of the inelastic curvatures of the plate, we revisit the phenomena of bistability of unsymmetric laminate composite and we discuss qualitatively the possible actuation modes for controlling the passage between one stable equilibrium configuration and the other by using embedded active layers. Namely, besides the well-documented snap-through phenomenon that can be induced with a single parameter actuation, we show that using two independent actuating parameters is possible to let the plate pass form one stable configuration to the other in a purely quasi-static fashion, following a path of stable equilibria. The third part presents an applicative example of the proposed actuation technique using a uniform composite plate including active layers of piezoelectric fiber composites. The aim here is two-fold: (i) to assess the technical feasibility of the proposed concepts, giving the typical order of magnitude of the values of the physical parameters and the technologic constraints; (ii) to validate the analysis performed with the simple uniform curvature model including only the first-order non-linear effects by fully-nonlinear finite element results obtained with a commercial finite element code.

2 UNIFORM CURVATURE VON KARMAN MODEL OF COMPOSITE PLATES

2.1 *Kinematics*

Consider a plate $\mathcal{S}$ and let us label its material points by their cartesian coordinates (x, y) in a flat initial configuration. Let $u(x, y) \in \mathbb{R}^2$ and $w(x, y) \in \mathbb{R}$ denote respectively the in-plane and the transverse displacements of the point (x, y). In unshearable plate models, the deformations are represented by two 2×2 symmetric tensor fields, the in-plane extension $e = (e_x, e_y, 2e_{xy})^T$ and the curvature $k = (k_x, k_y, 2k_{xy})^T$; here and henceforth their components are listed in three components columns by using the standard Voigt notation. According to the von Karman kinematics, the compatibility relations between deformations and displacements read as:

$$
e_x(u, w) = \frac{\partial u_x}{\partial x} + \frac{1}{2}\left(\frac{\partial w}{\partial x}\right)^2, \quad e_y(u, w) = \frac{\partial u_y}{\partial y} + \frac{1}{2}\left(\frac{\partial w}{\partial y}\right)^2,
$$

$$
e_{xy}(u, w) = \frac{1}{2}\left(\frac{\partial u_x}{\partial y} + \frac{\partial u_y}{\partial x}\right) + \frac{1}{2}\left(\frac{\partial w}{\partial x}\frac{\partial w}{\partial y}\right), \tag{1}
$$

$$
k_x(w) = \frac{\partial^2 w}{\partial x^2}, \quad k_y(w) = \frac{\partial^2 w}{\partial y^2}, \quad k_{xy}(w) = \frac{\partial^2 w}{\partial x \partial y}.
$$

where the in-plane extension includes the first-order nonlinear geometric contribution due to transverse displacements. Equations (1) imply the following compatibility condition between the in-plane extension e and the curvature k:

$$
\mathcal{L}(e) := \frac{\partial^2 e_y}{\partial x^2} + \frac{\partial^2 e_x}{\partial y^2} - 2\frac{\partial^2 e_{xy}}{\partial x \partial y} = \det k, \tag{2}
$$

where $\det k = k_x k_y - k_{xy}^2$ is the Gaussian curvatures of the plate current configuration and $\mathcal{L}$ is a linear second-order differential operator. If (e, k) do not verify the equation above, equations (1) are not integrable. This means that it is impossible to find a configuration of the plate with the deformations (e, k), without cutting the plate in several pieces. The compatibility relation (2) is an extremely useful intrinsic statement of the coupling between in plane-extension and Gaussian-curvature. Especially, it shows that any change of Gaussian curvature implies a non-uniform in-plane extension.

2.2 Constitutive behavior and potential energy

The generalized stresses of a plate are represented by the symmetric tensor fields $\sigma = (\sigma_x, \sigma_y, \sigma_{xy})^T$ and $m = (m_x, m_y, m_{xy})^T$ the 2×2 representing the force and moment resultants of the contact actions across the plate thickness. Composites plates with linear constitutive behavior are characterized by the following constitutive relations

$$\sigma(e,k) = \bar{A}\,(e - e_R) \ + \overline{B}\,(k - k_R)\,, \tag{3}$$

$$m(e,k) = \overline{B}^T\,(e - e_R) + \overline{D}\,(k - k_R)\,, \tag{4}$$

where $\bar{A}$, $\overline{B}$, and $\overline{D}$ are the standard 3×3 matrices of composite plate theory, representing in the Voigt notation the extensional stiffness, the extension-to-bending coupling, and the bending stiffness, respectively. Equations (4) account for the fact that the initial flat configuration with $e = 0$, $k = 0$ may be not stress-free. The tensors $e_R = (e_{Rx}, e_{Ry}, 2\,e_{Rxy})^T$ and $k_R = (k_{Rx}, k_{Ry}, 2\,k_{Rxy})^T$ stay for the plate deformation in a *relaxed* stress-free stance; they may be used to model the effect of inelastic deformations, as thermal or plastic deformations, and deformations induced by active materials, as piezoelectrics. Note that the relaxed stance may be a geometrically unreachable configuration, because e_R and k_R need not to satisfy the implicit compatibility condition (2). Our analysis will be restricted to the case where k_R is constant in space. We allow for non-constant in-plane inelastic deformations e_R, but we assume that they are such that the corresponding gaussian curvature $\mathcal{L}(e_R)$ is constant.

For the following developments is useful to introduce the bending stiffness at $\sigma = 0$, say $\widetilde{D}$, which is calculated to be $\widetilde{D} = \overline{D} - \overline{B}^T \bar{A}^{-1} \overline{B}$. We further define its non-dimensional version as $D := \widetilde{D}/\widetilde{D}_{11}$. For orthotropic plates, D may be written in the form :

$$D = \begin{bmatrix} 1 & \nu & 0 \\ \nu & \beta & 0 \\ 0 & 0 & \varrho \end{bmatrix}, \tag{5}$$

where $\beta = \widetilde{D}_{22}/\widetilde{D}_{11}, \nu = \widetilde{D}_{12}/\widetilde{D}_{11}, \rho = \widetilde{D}_{33}\widetilde{D}_{22}/(\widetilde{D}_{11}\widetilde{D}_{22} - \widetilde{D}_{12}^2), \varrho = \widetilde{D}_{33} = \rho \left(1 - \dfrac{\nu^2}{\beta}\right)$. We look for the shapes of the stable equilibrium configurations as a function of the inelastic deformation e_R and k_R, which we regard as control parameters. For plates without applied forces, the total potential energy reads as

$$\mathcal{U}(u,w) = \quad \frac{1}{2} \int_{\mathcal{S}} \bar{A}\,(e(u,w) - e_R) \cdot (e(u,w) - e_R)\,d\bar{S} +$$

$$+ \int_{\mathcal{S}} \overline{B}^T\,(e(u,w) - e_R) \cdot (k(w) - k_R)\,d\bar{S} + \tag{6}$$

$$+ \frac{1}{2} \int_{\mathcal{S}} \overline{D}\,(k(w) - k_R) \cdot (k(w) - k_R)\,d\bar{S},$$

where e and k are given by (1) and $d\bar{S}$ is the surface element. The first term of (6) is the extensional energy, the third term is the bending energy, and the second term is due to bending-extension coupling. The stable equilibria are then defined as the local minimizers of (6) in the spaces of admissible in plane and transverse displacements u and w.

2.3 *Uniform curvature hypothesis and intrinsic model in terms of curvatures*

Focusing on plates free at the boundaries, without applied forces, and with uniform inelastic curvatures k_R, we look for approximate analytical solutions by introducing the key hypothesis that the curvature k is constant throughout the plate, i.e. that

$$w = w_k(x, y) := 1/2\,k_x\,x^2 + 1/2\,k_y\,y^2 + k_{xy}\,x\,y, \tag{7}$$

with constant k_x, k_y, and k_{xy}. By using the hypothesis (7), the potential energy may be rewritten as

$$\widetilde{\mathcal{U}}(u, k) = \frac{1}{2}\,\bar{S}\,\widetilde{D}\,(k - k_R) \cdot (k - k_R) + \frac{1}{2}\int_{\mathcal{S}} \bar{A}^{-1}\,\sigma \cdot \sigma\, d\bar{S}, \tag{8}$$

where $\widetilde{D}$ is the bending stiffness at null in-plane stress, $\bar{S}$ is the surface of the plate, and

$$\sigma = \bar{A}(e(u, w_k) - e_R) + \overline{B}\,(k - k_R)\,. \tag{9}$$

The stable equilibria are now the minima of (8) with respect to u and k. Yet, one can solve the membranal problem to obtain an intrinsic discrete model in terms of curvature only.

The stationarity condition with respect to u gives the in-plane equilibrium equations:

$$\operatorname{div}\sigma = 0 \quad \text{on} \quad \bar{S} \qquad \text{and} \qquad \sigma\,n = 0 \quad \text{on} \quad \partial\bar{S}, \tag{10}$$

where n is the normal to the boundary $\partial\mathcal{S}$, supposed to be free. Equations (10) together with the constitutive equations (9) and the compatibility conditions (1) constitutes a classical *linear* problem of plane linear elasticity, which may be solved uniquely as a function of k. For the present case of a free plate in which there are not boundary conditions on the displacement field, the in-plane problem may be conveniently reformulated in terms of stresses, by using the implicit version (2) of the compatibility equation. For an homogeneous plate with uniform $\bar{A}$, $\overline{B}$, k, and k_R, solving (9) with respect to e, substituting into (2), and accounting for the linearlity of $\mathcal{L}$ gives:

$$\mathcal{L}(\bar{A}^{-1}\sigma) = \det k - \mathcal{L}(e_R). \tag{11}$$

The right-hand side of equation (11) is the difference between the actual gaussian curvature and the gaussian curvature associated to the in-plane inelastic deformations e_R. If $\mathcal{L}(e_R) = 0$, as obtained for uniform inelastic in-plane deformations, the only forcing term of the linear system of equation (10-11) for the in-plane problem is $\det k$ and the solution for σ must be in the form:

$$\sigma = \frac{\widetilde{D}_{11}L^2}{t^2}\,\Sigma(x,\,y)\,\det k, \tag{12}$$

where $L := \sqrt{\bar{S}}$ is the typical in-plane dimension of the plate and $\Sigma(x,\,y)$ is a non-dimensional function giving the stress distribution, being defined as the solution of the boundary value problem (11-10) for $\det k = t^2/\widetilde{D}_{11}L^2$.

Substituting the solution for in-plane problem in the form (12) into (8) gives an expression for the energy in terms of the curvature only. Here, we define the non-dimensional actual and inelastic curvatures $K = \{K_x, K_y, 2K_{xy}\}$ and $H = \{H_x, H_y, 2H_{xy}\}$ by adopting the scaling:

$$(K_x, H_x) = R_0\,(k_x, k_{Rx}), \quad (K_y, H_y) = R_0\,\sqrt{\beta}\,(k_y, k_{Ry}), \quad (K_{xy}, H_{xy}) = R_0\,\sqrt[4]{\beta}\,(k_{xy}, k_{Rxy}), \tag{13}$$

and choosing the scaling radius of curvature as:

$$R_0 := \frac{L^2}{t}\,\psi \quad \text{with} \quad \psi := \sqrt{\int_{\mathcal{S}} A^{-1}\,\Sigma \cdot \Sigma\, dS}, \tag{14}$$

where $dS := d\bar{S}/L^2$ and $A := \bar{A}_{11}t^2/\widetilde{D}_{11}$ are the non-dimensional element of area and extensional stiffness. With this scaling, the non-dimensional version of the energy function (8) simplifies to

$$U(K) = \frac{1}{2}\,D^*\,(K - K_R) \cdot (K - K_R) + \frac{1}{2}\,(\det K)^2\,, \quad D^* = \begin{bmatrix} 1 & \mu & 0 \\ \mu & 1 & 0 \\ 0 & 0 & \gamma \end{bmatrix}. \tag{15}$$

D^* is a bending stiffness matrix for a material with the same stiffness in the two principal directions, equivalent Poisson ratio μ, and non-dimensional shear modulus γ defined as:

$$\mu = \frac{\nu}{\sqrt{\beta}}, \quad \gamma = (1 - \mu^2)\frac{\varrho}{\sqrt{\beta}}. \tag{16}$$

The stable equilibria of the plate under the uniform curvature hypothesis may be obtained by minimizing $U(K)$ for $K = (K_x, K_y, 2K_{xy})^T \in \mathbb{R}^3$. This problem is purely algebraic and may be tackled analytically. The non-uniform scaling (13) has the merit of reducing the problem for a generic orthotropic plate to the one for an equivalent square symmetric composite. Especially, this clearly shows that there are only two relevant material parameters for the study of uniform curvature solution of orthotropic Von Karman plates: μ and γ. The ratios between the Young moduli in the two coordinate directions, β is tantamount to a rescaling of the curvatures.

3   EQUILIBRIA AND STABILITY

We study how the equilibria of the plate and their stability properties depend on the inelastic curvatures H_x and H_y, supposing $H_{xy} = 0$. In the proposed uniform curvature model, the equilibria are the points of stationarity of (15), *i.e.* the solutions of:

$$K_x - H_x + \nu(K_y - H_y) + K_y \det K = 0, \tag{17a}$$
$$\beta\,(K_y - H_y) + \nu(K_x - H_x) + K_x \det K = 0, \tag{17b}$$
$$2\,K_{xy}\,(\det K - 2\,\varrho) = 0, \tag{17c}$$

where $\det K = K_x K_y - K_{xy}^2$ is the gaussian curvature of the plate, the source of nonlinearity in the system behaviour. The stability of an equilibrium position K depends on the sign of the hessian matrix

$$\frac{\partial^2 U}{\partial K^2} = \begin{pmatrix} K_y^2 + 1 & 2K_x K_y + \nu - K_{xy}^2 & -2K_{xy}K_y \\ 2K_x K_y + \nu - K_{xy}^2 & K_x^2 + \beta & -2K_{xy}K_x \\ -2K_{xy}K_y & -2K_{xy}K_x & 6K_{xy}^2 + 4\varrho - 2K_x K_y \end{pmatrix}. \tag{18}$$

When the matrix is positive (negative) definite the equilibrium is stable (unstable). Remarkably in the present case the stability depends only on the position in the state space $K_x - K_y$, the hessian being indipendent of the control parameters H_x and H_y. Some properties of the solutions of the nonlinear system of equations (17) may be deduced by looking at the third equilibrium equation, which implies that either $K_{xy} = 0$ or $\det K = 2\,\varrho$. In other words equilibria for $H_{xy} = 0$ may

5
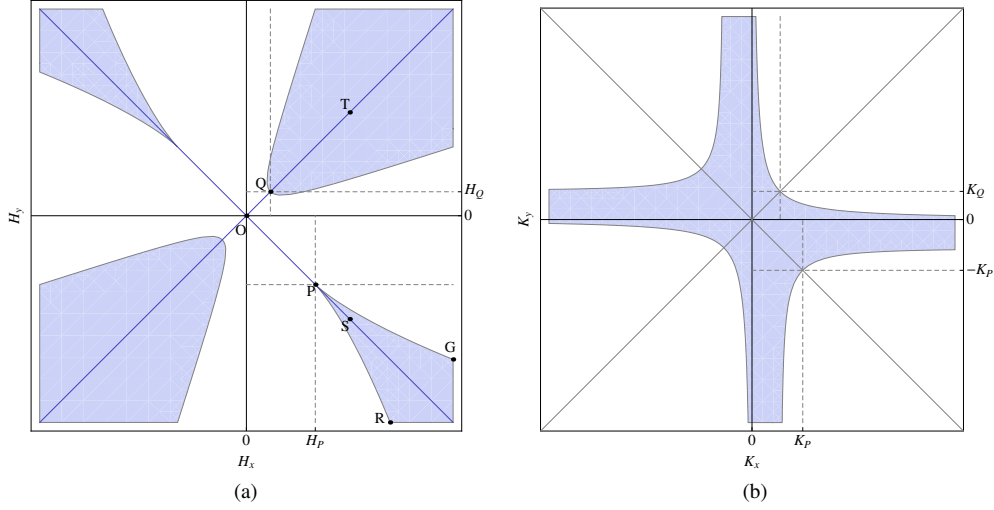
Figure 1: Stability diagram in the $H_x - H_y$ plane (a) and in the $K_x - K_y$ plane (b).

be untwisted or twisted, but the twisted ones are with assigned gaussian curvature. The following discussion distinguishes the two cases.

The equilibrium equations for the untwisted equilibria, $K_{xy} = 0$, are nonlinear in K_x and K_y. Yet, their stability is rather simple to be studied: applying the Sylvester's criterion to the hessian matrix (18) with $K_{xy} = 0$, one can show that the untwisted equilibria are stable if the following two conditions are satisfied:

$$\left(1 + K_y^2\right)\left(\beta + K_x^2\right) - \left(2\,K_x\,K_y + \nu\right)^2 > 0, \tag{19a}$$

$$2\,\varrho - K_x K_y > 0. \tag{19b}$$

In the special case of equal or opposite inelastic curvatures H_x, H_y, closed-form solutions for the untwisted equilibria are available. Namely, for $H_x = h$ and $H_y = \pm h$, we find three solution of the equilibrium equation, say $K^{(1)}$, $K^{(2)}$, and $K^{(3)}$, given by

$$K_x^{(1)} = \pm K_y^{(1)} = 2\frac{\sqrt[3]{2}\ \sqrt[3]{f^2(h, \pm\nu)} - 2\sqrt[3]{3}(1 \pm \nu)}{6^{2/3}\sqrt[3]{f(h, \pm\nu)}}, \tag{20a}$$

$$K_x^{(2)} = K_y^{(3)} = h(1 \pm \nu) + \sqrt{h^2(1 \pm \nu)^2 - 4(1 \mp \nu)} \tag{20b}$$

$$K_y^{(2)} = K_x^{(3)} = h(1 \pm \nu) - \sqrt{h^2(1 \pm \nu)^2 - 4(1 \mp \nu)} \tag{20c}$$

where $f(h, \nu) = (1 + \nu)\left(\sqrt{3}\sqrt{27h^2 + 4(1 + \nu)} + 9h\right)$. The first equilibrium $K^{(1)}$ is always real; the second and third equilibrium, $K^{(2)}$ and $K^{(3)}$, are real for $|h| \geq h_c$, with $h_c = 2\sqrt{1 \mp \nu}/(1 \pm \nu)$. For $h = h_c$ the three equilibria coalesce at the critical point $K_x = \pm K_y = \pm k_c$ with $k_c = \sqrt{\mu + 1}$.

The solution for the twisted equilibria $K_{xy} \neq 0$ is simple because they are with assigned gaussian curvature $\det K = 2\,\varrho$. Using this property, the equilibrium equations become linear in K_x and K_y

and may be solved to get:

$$K_x = \frac{H_x(\beta - \nu(\nu + 2\varrho)) - 2\beta\varrho H_y}{\beta - (\nu + 2\varrho)^2}, \tag{21a}$$

$$K_y = \frac{H_y(\beta - \nu(\nu + 2\varrho)) - 2\varrho H_x}{\beta - (\nu + 2\varrho)^2}, \tag{21b}$$

$$K_{xy} = \pm\sqrt{K_x K_y - 2\varrho}. \tag{21c}$$

These kind of equilibria are real only if $K_x K_y > 2\varrho$. In particular, plates with negative Gaussian curvature admit only untwisted equilibria if $H_{xy} = 0$.

Figures 1 illustrates the behaviour of the system, reporting (a) the partition of the state space $K_x - K_y$ in stability regions according to the criteria (19) and (b) the phase portrait of the system as a function of the inelastic curvature $H_x - H_y$, which distinguishes among regions of bistability (gray) and monostability (white).

4   ACTUATION OF BISTABLE PLATES

In this section we analyze possible actuation techniques of bistable plates at the light of the global stability analysis presented above. The aim is to determine how is possible to induce the passage between the two stable configurations of the plate by controlling the inelastic curvatures.

We focus on bistable plates with negative gaussian curvatures. Let us assume that initially the plate has an inelastic curvature H_A, as at the point A of figure 2a. It is then bistable with the two stable equilibria A_1 and A_2 in figure 2b. The inelastic curvature H_A may be due to plastic deformations or thermal effects. For example, it may be obtained by curving two times over the elastic regime a thin square aluminum plate: one time by bending it in one direction and one sense, one time in the opposite direction and opposite sense. Another well-studied class of structures showing this kind of initial curvatures are composite plates made of unsymmetric laminates [5]. In this case, the inelastic curvatures are due to thermal strains induced during the curing process. We suppose that we are able to control the inelastic curvatures H_x and H_y around H_A. In particular, by using composite plates including piezoelectric fibers [11], or smart memory alloys wires, it is possible to conceive system configurations allowing to control the inelastic curvatures in the two coordinate directions by two independent control parameters.

Several authors investigated the use of a piezoelectric actuator to control the transition between the two equilibria of the bistable plate [11, 12]. The effect of a single actuator made of piezoelectric fiber composite may be considered equivalent to an induced inelastic curvature applied along a specific direction, say H_y, which will add to the initial inelastic curvature H_1. In piezoelectric composites, this curvature is controlled by the applied voltage. Referring to figure 2a, the piezoelectric induced curvature may be used to change the total inelastic curvature from H_A along the line AE. If the system configuration is initially in the state A_1 of figure 2b, when moving the control curvature along AE, the actual configuration of the plate moves along the curve A_1F_1 of figure 2b. When the inelastic curvature reach the boundary of the bistability region at point F, the current configuration becomes unstable; thus the plate snap-through to the other possible equilibrium F_2 which stay stable. When releasing the added actuation, the inelastic curvature come back to H_A, but the plate holds now the equilibrium position A_2. This kind of passage between the configurations $A_1 \rightarrow A_2$ happens dynamically, with a snap-through phenomenon.

On the contrary, having two independent control parameters offers novel possibilities to induce the passage between the equilibria $A_1 \rightarrow A_2$. A fundamentally new type of transition is obtained
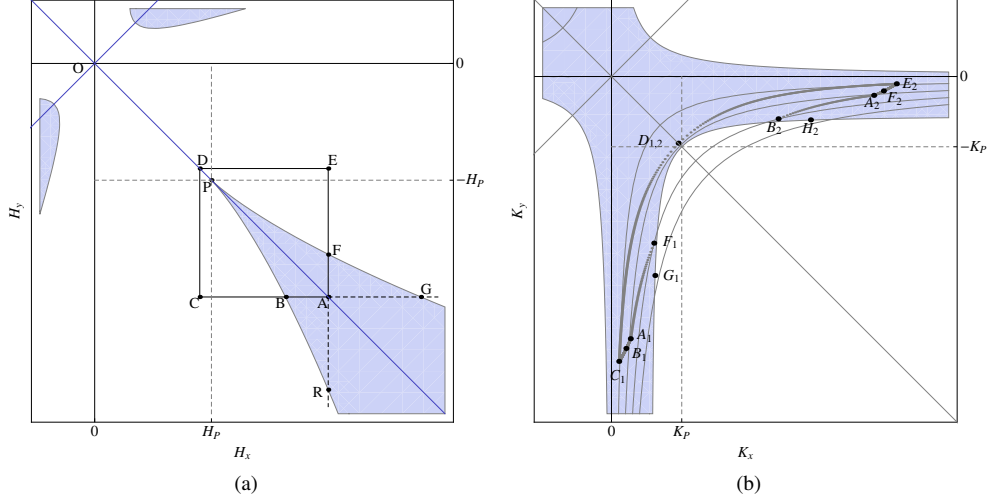
Figure 2: Stability diagrams and stable $R - K$ paths.

by using an actuation path circumventing the cusp point P. A simple example is the path ACDEA in figure 2a, composed of four steps: (i) a negative change, say ΔH of the inelastic curvature in the x direction, (ii) a positive change ΔH of the inelastic curvature in the y direction, (iii) a positive change ΔH of the inelastic curvature in the x direction, and finally (iv) a negative change, say ΔH of the inelastic curvature in the x direction which restore the initial inelastic curvature H_A. Assuming that the plate is initially in the configuration A_1, when following this path, the current configuration of the plat moves along the path $A_1C_1D_1E_2A_2$ in figure 2b. As with the single-parameter actuation one obtains the passage $A_1 \rightarrow A_2$, the plate being able to hold the two configurations without actuation. But there is a fundamental different in the way in which the transition is obtained: the configuration A_2 is reached in a purely quasi-static way, without any kind of instability and dynamic phenomenon. Indeed, the system configuration remains within the stability region of figure 2b.
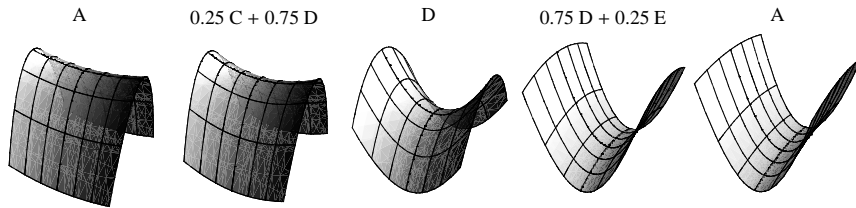
Figure 3: Plates shapes along a closed clockwise path from A to A surrounding the cusp point P.

Figure 3 shows the shapes assumed when the plate starts from configuration A_1 and the relaxed stance is varied linearly from point A, to point $0.25C + 0.75D$, then to point D, then to point $0.75D + 0.25E$ and finally back to point A. When starting from $K = A_2$ and reverting the previous path for the relaxed stance, will obviously lead the plate in the configuration A_1 by a stable transition.

8
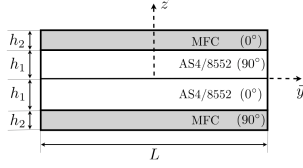
Figure 4: Cross-sectional geometry of the square composite plate.

	E_1 (GPa)	E_2 (GPa)	G_{12} (GPa)	G_{13} (GPa)	G_{23} (GPa)	ν_{12}	α_1 (10^{-6}/°C)	α_2 (10^{-6}/°C)
AS4/8552	135.	9.5	5.	7.17	3.97	0.3	-0.02	$-30.$

Table 1: Mechanical properties of the AS4/8552.

5 APPLICATIVE EXAMPLE AND FINITE ELEMENT VALIDATION

To validate the results of the uniform curvature model and to present the technological feasibility of the multiparameter actuating technique proposed, we consider finite element results for an applicative example consisting of unsymmetric cross-ply [0°/90°] composite laminate made from AS4/8552 with two thin layers of Macro-Fiber Composite (MFC) actuators bonded to its top and bottom surfaces (Figure 4). The MFC actuator consists of piezoelectric fibers embedded in an epoxy matrix and is actuated using interdigitated electrodes. The composite plate is assembled at high temperature and then cooled down. The MFC layers are glued on the plate after the curing process either in the curved configuration or bonding the actuator on the composite beneath a weight to keep the composite and actuator flat. The MFC are supposed to cover the entire plate surface.

To simulate this system in the finite element code ABAQUS using shell elements, we bonded together three shells using the *TIE constraint. The central shell represents the [0°/90°] composite laminate, the top and bottom shells stay for the MFC actuators. This kind of configuration allows us to introduce layerwise inelastic strain through three independent parameters: one associated to the temperature of the central plate, the other two with the voltages of the top and bottom piezoelectric layers. For sake of simplicity, our finite element simulations model the curing process by applying an uniform temperature gradient (ΔT) to elastic layers only. The lenght of the square plate is $L = 25cm$ and the thickness of composite layers is $h_1 = 0.36mm$ whilst that of MFC layers is $h_2 = 0.3mm$. The properties of AS4/8552 and MFC materials are listed respectively in Table 1 and 2.

To take into account of the piezoelectric effect in the finite element simulations, the free-strain per volt $\beta_1 = 0.75\mu\varepsilon/V$, relation between applied voltage and strain given by the manufacture of the MFC, is introduced as a thermal expansion coefficient. Applying a temperature field (ΔT) to MFC layers in ABAQUS thus corresponds to apply a voltage (ΔV). A quasistatic finite element simulation is made to reproduce the multiparametric path $ABCDEA$ in Figure 2(a). The different loadings were applied in five steps, corresponding to the application of the different inelastic curvatures on Figure 2(a). Figure 5 shows a noticeable agreement between the finite element results (dashed) and the analytical results (solid) for the average curvatures K_x et K_y along the path $OACDEA$.

	E_1 (GPa)	E_2 (GPa)	G_{12} (GPa)	ν_{12}	β_1 ($10^{-6}\varepsilon$/V)
MFC	30.34	15.86	5.52	0.31	0.75

Table 2: Mechanical properties of the MFC actuator.

9
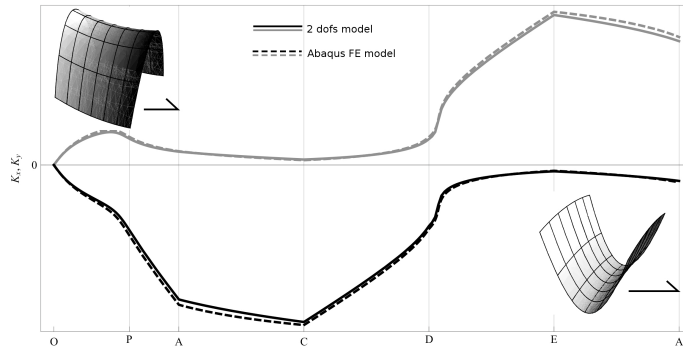
Figure 5: Comparison of average curvatures K_x (black) et K_y (grey) on path $OACDEA$

References

[1] Bowen, C., Butler, R., Jervis, R., Kim, H., Salo, A., Morphing and shape control using unsymmetrical composites, *J. Intelligent Material Systems and Structures* **18**, 89–98 (2007).

[2] Calladine, C., *Theory of shell structures*, Cambridge, UK: Cambridge University Press (1983).

[3] Di Carlo, A., Quiligotti, S., Growth and balance, *Mech. Res. Comm.* **29**, 449–456 (2002).

[4] Guest, S., Pellegrino S., Analytical models for bistable cylindrical shells, *Proc. Royal Society A* **462**(2067), 839–854 (2006).

[5] Hyer, M. W., Calculation of the room-temperature shapes of unsymmetric laminates, *J. Composite Materials* **15**, 296–310 (1981).

[6] Kebadze, E., Guest, S., Pellegrino, S., Bistable prestressed shell structures, *Int. J. Solids and Structures* **41**(11-12), 2801–2820 (2004).

[7] Mansfield, E. H., Bending, buckling and curling of a heated thin plate, *Proc. Royal Society Series A* **268**(1334), 316–327 (1962).

[8] Mattioni, F., Weaver, P., Potter, K., Friswell, M., Analysis of thermally induced multistable composites, *Int. J. Solids and Structures* **45**, 657–675 (2007).

[9] Maurini, C., Pouget, J., Vidoli, S., Distributed piezoelectric actuation of a bistable buckled beam, *Eur. J. Mechanics - A/Solids* **26**, 837–853 (2007).

[10] Vidoli, S., Maurini, C., Tristability of thin orthotropic shells with uniform initial curvature, *Proc. Royal Society A***464**(2099), 2949–2966 (2008).

[11] Portela, P., Camanho, P., Weaver, P., Bond, I., Analysis of morphing, multi stable structures actuated by piezoelectric patches, *Computers & Structures*, **86**(3-5), 347–356 (2008).

[12] Schultz, M. R., Hyer, M., Williams, R., Wilkie, W., Inman, D., Snap-through of unsymmetric laminates using piezocomposite actuators, *Composite Science Tech.* **15**, 296–310 (2006).

[13] Seffen, K. A., 'Morphing' bistable orthotropic elliptical shallow shells, *Proc. Royal Society A* **463**(2077), 67–83 (2007).